CHAPTER 5

DYNAMICS OF FLEXIBLE SPACECRAFT

5.1 INTRODUCTION

In this chapter we illustrate a number of methods which can be used to obtain the equations of motion for vehicles which are modeled as an elastic continuum. Since the subject of modeling theory (for multibody satellite dynamics) is a distinct engineering discipline in its own right (ref. 1-45), we focus attention in this chapter on elementary modeling techniques and a specific spacecraft configuration, in order to capture the essential ideas. Appropriate extensions for handling more general, near-arbitrary systems of interconnected flexible bodies can be found in References 7, 15 through 24, 28, and 29.

Since flexible spacecraft are most rigorously modeled as distributed parameter systems, their motion is most fundamentally described by partial differential equations. Unfortunately, coupled partial differential equation models are difficult to deal with both analytically and computationally, vis-a-vis applications to realistic spacecraft. As a result, we are usually forced to apply more versatile methods leading to more easily handled, approximate equations of motion. There are many popular misconceptions on the subject of discrete (ordinary differential equation) models versus distributed or continuous (partial differential equation) models. The extreme positions have both the distributed system and discretized system advocates claiming the other camp is making hopelessly naive approximations of reality. Truth lies in the insight that neither approach *guarantees* a reasonable approximation of a given "real" dynamical system. Both viewpoints require substantial "artwork" to obtain practical results. There can be little doubt, however, that a large fraction of the applications ultimately demand a spatial discretization. To this end, we present in this chapter several approaches for obtaining suitable approximate equations of motion for distributed parameters systems.

In Section 5.2 we describe the *hybrid coordinate* (discrete *and* continuous coordinates) formulation of the equations of motion. As an example of the hybrid coordinate formulation, the equations of motion for a simple space structure are developed in Section 5.3. The so-called foreshortening effect of deforming elastic structures is also presented in Section 5.3, this nonlinear effect is important in dynamical sistuations in which high angular rates are achieved.

Section 5.4 describes the two most common methods for discretizing the equations of motion; the finite element method, and the method of assumed modes. Also presented in Section 5.4 is a summary of the equations of motion for a multibody spacecraft which makes use of finite element modeling techniques to characterize the deformation of each elastic member.

5.2 THE HYBRID COORDINATE METHOD

The coordinates used to describe the motion of flexible vehicles are referred to as hybrid, because the vehicle's equations of motion consist of both ordinary and partial differential equations. The ordinary differential equations describe discrete coordinates which are used for modeling rotations and translations of the overall configuration and perhaps a set of substructures idealized as particles or rigid bodies. The partial differential equations, on the other hand, govern the behavior of distributed coordinates which are used for modeling the deformations of elastic bodies.

The issues associated with modeling potential disturbances are not easily stated or resolved. It is common practice to lump as "disturbances" all poorly understood and sometimes random events such as the following partial list:

- on-board disturbance forces and torques due to machinery operation and crew motion

- gravity-gradient torques
- propellant slosh
- aerodynamic forces and moments
- thermal loads
- solar radiation pressure
- control system, sensor, and actuator dynamics
- changes in the system configuration parameters due to deployment, expendable fuels, etc.

In some cases, near-deterministic simulation studies are possible if the frequency and amplitude content of the disturbance is well understood. In other cases, a random (stochastic) approach must be taken. In all cases, it is desired that the system performance be sufficiently "robust" in the presence of the actual disturbances likely to be experienced.

The procedure most commonly used for analyzing hybrid systems is a *spatial discretization*, whereby the partial differential equations are replaced by infinite sets of ordinary differential equations. A *reduced-order model* for the distributed parameter system is selected by truncating the infinite sets of ordinary differential equations based upon the requirements for individual applications. A frustrating truth is that no rigorous deterministic method exists to construct the reduced order model. The selection of a suitable reduced-order model is very important, because of the possibility of on-board control systems or external disturbances exciting a resonance condition. Indeed, failure to observe this truth can, in the worst case, lead to an unstable system.

Though a theoretical resolution of the truncation and disturbance modeling issues is not available at this time, this does not exclude ad hoc practical solution methods. Indeed, this situation is somewhat analogous to the impossibility of exact truncation/arithmetic error bounds when numerically solving complicated systems of nonlinear differential equations. The lack of complete analytical tractability is frustrating, but it does not keep us (for example) from confidently computing accurate earth-moon trajectories! There are numerous common-sense experiments one can conduct to build the insight and confidence necessary to bridge the gap between limitations of our theory and the practicalities of specific applications. The necessity of this artistic engineering in spacecraft dynamics and control is not in doubt; it is necessary (in fact, absolutely vital) no matter how sophisticated our modeling and control theory, especially for many degree of freedom dynamics and control problems.

Mathematically, one approach to spatial discretization (refs. 46, 49) is to model time and space variable defection of the continuous elastic members by a finite series of prescribed (admissible) space-dependent functions, which are multiplied by time-dependent generalized coordinates. This is essentially the Ritz Method (refs. 50, 51). Upon carrying out this process, the coordinates (whose time derivatives are governed by the equations of motion) include: (1) a set of the discrete coordinates for rigid body translations and rotations, and (2) the generalized coordinates arising in the spatial discretization procedure. The set of prescribed space-dependent functions typically consists of approximate structural mode shapes obtained from (1) a finite element model, or (2) experimental data, or (3) from an analytically tractable approximate dynamical model.

In particular, if approximate analytical mode shapes are used, the modeling technique is widely referred to as the "method of assumed modes" (refs. 46, 49). A basic requirement is that a complete set of linearly independent functjons must be used, these functions must satisfy geometric boundary conditions to qualify as admissible functions in the method of assumed

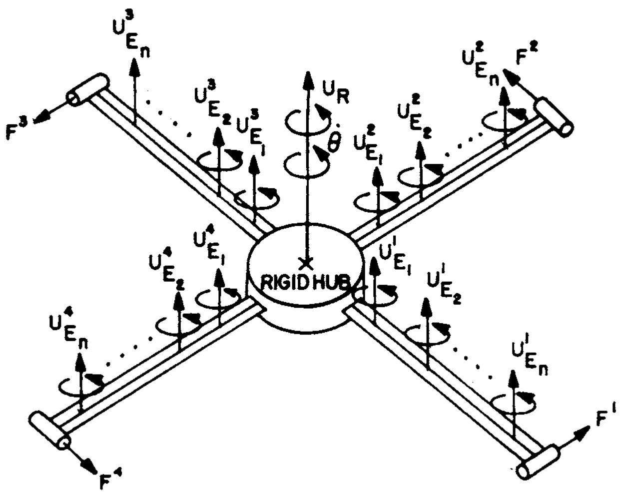

$U_R \triangleq$ RIGID HUB CONTROL TORQUE

$U_E \triangleq \left\{U^1_{E_1} \ldots U^1_{E_n} U^2_{E_1} \ldots U^2_{E_n} U^3_{E_1} \ldots U^3_{E_n} U^4_{E_1} \ldots U^4_{E_n}\right\}^T$

= ELASTIC APPENDAGE CONTROL TORQUES

$U_T \triangleq \left\{F^1 \ldots F^4\right\}^T$

= APPENDAGE TIP CONTROL THRUSTERS

Figure 5.1 Undeformed Structure

modes. Of course, as a by-product of the analysis, the actual normal modes are approximated by linear combinations of the assumed modes, and (in this sense) the method is poorly named.

5.3 EXAMPLE APPLICATION OF THE HYBRID COORDINATE METHOD

In order to bring various modeling issues into focus, it is useful to consider an example. The specific model considered in this section (Fig. 5.1) consists of a rigid hub with four identical elastic appendages attached symmetrically about the central hub. In particular, we make the following idealizations: (i) large-angle single-axis maneuvers; (ii) in-plane motion,

(iii) anti-symmetric deformations (Fig. 5.2); (iv) small linear flexural deformations (as seen in the rotating, hub-fixed reference frame); (v) nonlinear rotation/vibration coupling effects arising from rotational "stiffening" are considered; (vi) the control actuators are modeled as either concentrated force or torque generating devices and (vii) the control actuators are idealized as massless and internal actuator dynamics are neglected. The distributed control system for the vehicle is taken to consist of: (1) a single external torque actuator acting on the rigid hub; (2) an arbitrary number of torque actuators acting at points along each appendage; and (3) a force (thruster) actuator located at the tip of each appendage. For simplicity, we assume the actuators are reversible and are capable of smooth unbounded control input to the structure.

For the vehicle depicted in Figure 5.1, the equations of motion can be obtained from Hamilton's extended principle, Eq. 3.106 and alternatively, using the methods presented in References 44, 46, and 49. The extended Hamilton's principle is

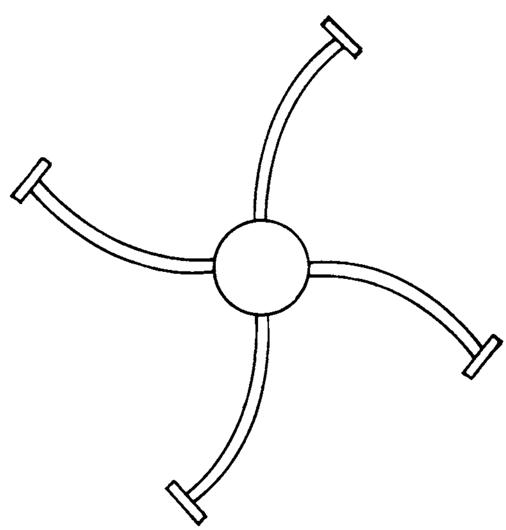

Figure 5.2 Antisymmetric Deformation of the Structure

$$\int_{t_1}^{t_2} (\delta L + \delta W)dt = 0 \tag{5.1}$$

subject to

$$\delta\theta = \delta u = 0 \text{ at } t_1,\ t_2$$

where $L = T - V$ is the system Lagrangian, δW is the virtual work, T is the kinetic energy, V is the potential energy, $\delta\theta$ is a virtual rigid body rotation, and $\delta u(x,t)$ is a virtual elastic deflection of a typical member, as measured in the hub-fixed coordinate system.

5.3.1 Virtual Work and Generalized Forces

The virtual work for the vehicle depicted in Figure 5.1 is

$$\delta W = \sum_{k=1}^{n} Q_k \, \delta q_k \tag{5.2}$$

where

$$Q_k = \int_V \frac{\partial \mathbf{R}^*}{\partial q_k} \cdot df, \tag{5.3}$$

$\mathbf{R}^*$ denotes the inertial position of a differential mass element, dm, in the vehicle (Figure 5.3), df denotes the differential resultant force acting on dm, q_k denotes the kth generalized coordinate, V denotes that the integration is taken over the entire vehicle, and n denotes the number of degrees of freedom in the equation of motion.

Referring to Figure 5.3, the following four steps are required in order to evaluate Eq. 5.3: first, we express the position vector $\mathbf{R}^*$ locating the differential mass element, dm, relative to an inertially fixed point O as

$$\mathbf{R}^* = \mathbf{R} + \mathbf{r} + \mathbf{u} \tag{5.4}$$

where the vector $\mathbf{R}$ locates relative to O the reference point P on the body; the vector $\mathbf{r}$ locates relative to P the undeformed position of the differential mass element, dm, where $\mathbf{r}$ is fixed in B; and the vector $\mathbf{u}$ locates relative to the terminus of $\mathbf{r}$ the deformed position of the differential mass element dm, where

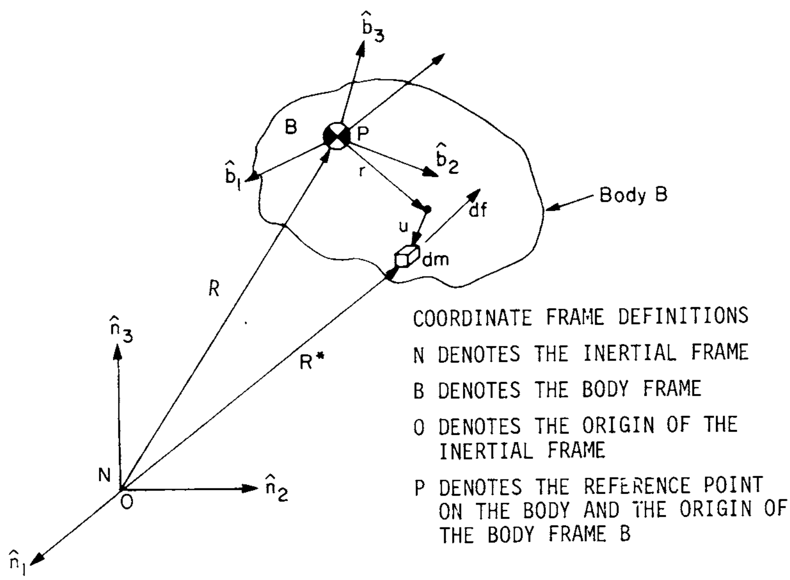

Figure 5.3 Deformation Notations for a General Body

$$\mathbf{u} = u_1(r_1,r_2,r_3,t)\hat{\mathbf{b}}_1 + u_2(r_1,r_2,r_3,t)\hat{\mathbf{b}}_2 + u_3(r_1,r_2,r_3,t)\hat{\mathbf{b}}_3$$

and

$$\mathbf{r} = r_1\hat{\mathbf{b}}_1 + r_2\hat{\mathbf{b}}_2 + r_3\hat{\mathbf{b}}_3$$

Second, using the "cancellation of dots" identity of Eq. 3.59, we observe that the expression for $\frac{\partial \mathbf{R}^*}{\partial q_k}$ in Eq. 5.3 can be replaced by

$$\frac{\partial \mathbf{R}^*}{\partial q_k} \stackrel{\Delta}{=} \frac{\partial}{\partial \dot{q}_k}\left(\frac{d}{dt}(\mathbf{R}^*)_N\right) \tag{5.5}$$

Third, in order to evaluate the required partial derivatives in Eq. 5.5, we substitute Eq. 5.4 into Eq. 5.5 and evaluate the inertial time derivative of Eq. 5.4 as follows

$$\frac{d}{dt}(\mathbf{R}^*)_N \stackrel{\Delta}{=} \frac{d}{dt}(\mathbf{R} + \mathbf{r} + \mathbf{u})_N = \frac{d}{dt}(\mathbf{R})_N + \frac{d}{dt}(\mathbf{u})_B + \omega \times (\mathbf{r} + \mathbf{u}) \tag{5.6}$$

Taking the partial derivative of Eq. 5.6 with respect to $\dot{q}_k$ yields

$$\frac{\partial}{\partial \dot{q}_k}\left(\frac{d}{dt}(\mathbf{R}^*)_N\right) = \frac{\partial \dot{\mathbf{R}}}{\partial \dot{q}_k} + \frac{\partial \mathring{\mathbf{u}}}{\partial \dot{q}_k} + \frac{\partial \boldsymbol{\omega}}{\partial \dot{q}_k} \times (\mathbf{r} + \mathbf{u}) \qquad (5.7)$$

where the dot over the vector **R** denotes differentiation in the inertial frame and the open circle over the vector **u** denotes differentiation in the body frame.

Substituting Eq. 5.7 into Eq. 5.3, and rearranging, we obtain

$$Q_k = \mathbf{f} \cdot \frac{\partial \dot{\mathbf{R}}}{\partial \dot{q}_k} + \frac{\partial \boldsymbol{\omega}}{\partial \dot{q}_k} \cdot \left[\int_V \mathbf{r} \times d\mathbf{f} + \int_V \mathbf{u} \times d\mathbf{f}\right] + \int_V \frac{\partial \mathring{\mathbf{u}}}{\partial \dot{q}_k} \cdot d\mathbf{f} \qquad (5.8)$$

where

$$\mathbf{f} = \int_V d\mathbf{f} = \int_{\text{Hub}} d\mathbf{f} + 4\int_{\text{Appendages}} d\mathbf{f} + 4\int_{\text{Thrusters}} d\mathbf{f}$$

Subject to the motion idealizations previously mentioned, the differential resultant forces, **df**, acting on the hub, appendages, and thrusters are summarized as follows:

Hub: $$d\mathbf{f} = -u_R \delta'(\mathbf{x})\hat{\mathbf{b}}_2 \qquad (5.9)$$

Appendages: $$d\mathbf{f} = -\sum_{i=1}^{n_E} u_{Ei}\delta'(\mathbf{x} - \mathbf{x}_{Ei})\hat{\mathbf{b}}_2 \qquad (5.10)$$

$$\mathbf{x}_{Ei} = x_i\hat{\mathbf{b}}_1 + u(x_i,t)\hat{\mathbf{b}}_2$$

Thrusters: $$d\mathbf{f} = -F\sin\left(\frac{\partial u}{\partial x}\Big|_{r+L}\right)\delta(\mathbf{x} - \mathbf{x}_T)\hat{\mathbf{b}}_1 + F\cos\left(\frac{\partial u}{\partial x}\Big|_{r+L}\right)\delta(\mathbf{x} - \mathbf{x}_T)\hat{\mathbf{b}}_2$$

$$\mathbf{x}_T = (r + L)\hat{\mathbf{b}}_1 + u(r + L,t)\hat{\mathbf{b}}_2 \qquad (5.11)$$

where

$\delta(\mathbf{x} - \mathbf{a}) = \delta(x_1 - a_1)\delta(x_2 - a_2)\delta(x_3 - a_3)$

$\delta'(\mathbf{x} - \mathbf{a}) = \delta'(x_1 - a_1)\delta'(x_2 - a_2)\delta'(x_3 - a_3)$

$\delta(x - b)$ denotes a delta function

$\delta'(x - b)$ denotes the spatial derivative of a delta function

u_R denotes the rigid body control torque

u_{Ei} denotes the ith appendage control torque

F denotes the thruster control force

$\frac{\partial}{\partial x}(\cdot)|_{r+L}$ denotes that the partial derivative of $(\cdot)$ is evaluated at $x = r + L$

Equations 5.9 and 5.10 can be verified by carrying out a limiting process in which an equivalent couple of a force pair is used to represent the moment applied at a point. Substituting Eqs. 5.9, 5.10, and 5.11 into Eq. 5.8, where

$$\mathbf{R} = 0,\ \mathbf{r} = x\hat{\mathbf{b}}_1,\ \mathbf{u} = u(x,t)\hat{\mathbf{b}}_2, \text{ and } \boldsymbol{\omega} = \dot{\theta}\hat{\mathbf{b}}_3$$

leads to

$$Q_k = \frac{\partial\dot{\theta}}{\partial\dot{q}_k}\left[u_R + \sum_{i=1}^{n_E} u_{Ei} + 4(r + L)F\cos\left(\frac{\partial u}{\partial x}\Big|_{r+L}\right) + 4u(r + \ell,t)F\sin\left(\frac{\partial u}{\partial x}\Big|_{r+L}\right)\right]$$
$$+ 4\sum_{i=1}^{n_E} \frac{\partial^2 \overset{\circ}{u}}{\partial\dot{q}_k\partial x}\Big|_{x_i} u_{Ei} + 4\frac{\partial\overset{\circ}{u}}{\partial\dot{q}_k}\Big|_{r+L} F\cos\left(\frac{\partial u}{\partial x}\Big|_{r+L}\right) \tag{5.12}$$

In order to complete the evaluation of Eq. 5.12 we first express $u(x,t)$ by the assumed modes method (Section 5.4) as the following series

$$u(x,t) = \sum_{i=1}^{n} \phi_i(x)\eta_i(t) \tag{5.13}$$

where $\phi_i(x)$ denotes the ith assumed mode shape, $\eta_k(t)$ denotes the kth generalized coordinate, and n denotes the number of terms retained in the approximation. The body frame time derivative of Eq. 5.13, required in Eq. 5.12, follows as:

$$\overset{\circ}{u}(x,t) = \sum_{i=1}^{n} \phi_i(x)\dot{\eta}_i(t)$$

As a result, in Eq. 5.12, the expressions for $\frac{\partial\dot{\theta}}{\partial\dot{q}_k}$, $\frac{\partial\overset{\circ}{u}}{\partial\dot{q}_k}$, and $\frac{\partial^2\overset{\circ}{u}}{\partial\dot{q}_k\partial x}\Big|_{x_i}$ are evaluated as follows

$$\frac{\partial\dot{\theta}}{\partial\dot{q}_k} = \begin{cases} 1\ , & \text{for } \dot{q}_k = \dot{\theta} \\ 0\ , & \text{for } \dot{q}_k \neq \dot{\theta} \end{cases} \tag{5.14}$$

$$\frac{\partial \overset{\circ}{u}}{\partial \dot{q}_k} = \begin{cases} \phi_k|_{r+L} & , \text{ for } \dot{q}_k = \dot{\eta}_k \\ 0 & , \text{ for } \dot{q}_k \neq \dot{\eta}_k \end{cases}$$

and

$$\frac{\partial^2 \overset{\circ}{u}}{\partial \dot{q}_k \partial x}\Big|_{x_i} = \begin{cases} \frac{\partial \phi}{\partial x}\Big|_{x_i} & , \text{ for } \dot{q}_k = \dot{\eta}_i \\ 0 & , \text{ for } \dot{q}_k \neq \dot{\eta}_i \end{cases} \tag{5.15}$$

5.3.2 Kinetic Energy

The system kinetic energy for the vehicle depicted in Figure 5.2 is

$$T = T_{Hub} + 4\, T_{Appendage} \tag{5.16}$$

where

$$T_{Hub} \overset{\Delta}{=} \frac{1}{2} I_{Hub}\, \dot{\theta}^2,$$

$$T_{Appendage} \overset{\Delta}{=} \frac{1}{2} \int_r^{r+L} \left| \frac{d}{dt} (\mathbf{R})_N \right|^2 dm,$$

I_{Hub} denotes the moment of inertia of the hub, $dm = \rho ds$, ρ denotes the constant linear mass density (per unit length), and ds denotes differential arc-length along an appendage.

In order to evaluate the integral for $T_{Appendage}$, we observe that $\mathbf{R}$ can be written as

$$\mathbf{R} = x\hat{\mathbf{b}}_1 + u(x,t)\hat{\mathbf{b}}_2$$

which leads to

$$\frac{d}{dt} (\mathbf{R})_N = \frac{d}{dt} (\mathbf{R})_B + {}^N\boldsymbol{\omega}^B \times \mathbf{R}$$

$$= -\,\dot{\theta} u \hat{\mathbf{b}}_1 + (\dot{u} + \dot{\theta} x)\hat{\mathbf{b}}_2$$

and

$$\left|\frac{d}{dt} (\mathbf{R})_N\right|^2 = \dot{\theta}^2 u^2 + \dot{u}^2 + 2x\dot{u}\dot{\theta} + \dot{\theta}^2 x^2$$

As a result, the integral for $T_{Appendage}$ can be written as

$$T_{Appendage} = \frac{\rho}{2} \int_r^{r+L} (\dot{\theta}^2 u^2 + \dot{u}^2 + 2x\dot{u}\dot{\theta} + \dot{\theta}^2 x^2) ds \tag{5.17}$$

The evaluation of Eq. 5.17 is complicated by the presence of both the position coordinate, x, and the arc length coordinate, s. In order to carry out the integration in Eq. 5.17, we can pursue one of two traditional paths: (1) we can assume that u and $\dot{\theta}$ are extremely small, which justifies the approximation $s = x$; or (2) we can obtain an expression which defines x as a function of s, that is $x = x(s)$. We choose the latter option since, in some of the maneuvers discussed in Chapter 9, large deflections and high angular rates are achieved (in which case, we'll find distinguishing between s and x is important). In particular, the expression relating x to s accounts for the so-called fore-shortening effect of the deforming elastic appendages which results in a given mass element having a variable distance from the mass center as a consequence of deformation. It is obvious that failure to distinguish between s and x implicitly results in unintended, differential "stretching or compression" of the appendage.

To find a suitable expression for x(s), we first observe the following definition for arc-length

$$ds = \sqrt{(dx)^2 + (dy)^2} = \sqrt{1 + \frac{1}{2}\left(\frac{\partial y}{\partial x}\right)^2}\, dx$$

By assuming that $\frac{\partial y}{\partial x}$ is small, the binomial theorem provides the first-order expression:

$$ds = \left[1 + \frac{1}{2}\left(\frac{\partial y}{\partial x}\right)^2\right] dx$$

Upon integrating the expression above for ds, we find

$$s = x + \delta x(x) \tag{5.18}$$

where $\delta x(x) = \frac{1}{2}\int_r^x \left(\frac{\partial y}{\partial x}\right)^2 dx$, $y = u(x,t)$, and $\delta x \sim O(u^2)$. By solving Eq. 5.18 for x, we obtain the desired result; namely:

$$x = s - \delta x(x) \tag{5.19}$$

Before introducing Eq. 5.19 into Eq. 5.17, we note the following relationships between u, $\frac{\partial y}{\partial x}$, and δx:

$$u(x) = u(s) + O(u^3)$$

$$\frac{\partial u}{\partial x} = \frac{\partial u}{\partial s} + O(u^3)$$

$$\delta x = \frac{1}{2}\int_r^s \rho(\frac{\partial u}{\partial s})^2 \, ds + O(u^4)$$

As a result, the kinetic energy, Eq. 5.17 can be written as

$$T_{Appendage} = \frac{\rho}{2}\int_r^{r+L} (\dot{\theta}^2u^2 + \dot{u}^2 + 2s\dot{u}\dot{\theta} + s^2\dot{\theta}^2 - 2\dot{\theta}^2 s\, \delta x(s))ds + O(u^3) \tag{5.20}$$

To simplify Eq. 5.20, we integrate the term containing δx by parts, as follows:

$$-2\dot{\theta}^2 \int_r^{r+L} s\delta x(s)ds = -2\dot{\theta}^2 \int_r^{r+L} s(\frac{1}{2}\int_r^s (\frac{\partial u}{\partial s'})^2 ds')ds$$

$$= -2\dot{\theta}^2[UV|_r^{r+L} - \int_r^{r+L} VdU]$$

where

$$U \triangleq \frac{1}{2}\int_r^s (\frac{\partial u}{\partial s'})^2 ds' \; ; \; V = \frac{1}{2} s^2;$$

$$dU \triangleq \frac{1}{2}(\frac{\partial u}{\partial s})^2|_s \qquad ; \; dV = sds$$

Thus

$$-2\dot{\theta}^2 \int_r^{r+L} s\delta x ds = -2\dot{\theta}^2 \int_r^{r+L} \frac{1}{4}[(r + L)^2 - s^2](\frac{\partial u}{\partial s})^2 ds$$

and Eq. 5.20 can be written in the final form as

$$T_{Appendage} \triangleq \frac{\rho}{2}\int_r^{r+L} [\dot{\theta}^2(s^2 + u^2 - p^2) + \dot{u}^2 + 2s\dot{u}\dot{\theta}]ds \tag{5.21}$$

where

$$p^2 = \frac{1}{2}[(r + L)^2 - s^2](\frac{\partial u}{\partial s})^2$$

5.3.3 Potential Energy

The potential energy for the vehicle depicted in Figure 5.1 can be shown to be

$$V = 4V_{Appendage} \tag{5.22}$$

where

$$V_{\text{Appendage}} = \frac{1}{2} \int_{r}^{r+L} EI[\frac{\partial^2 u}{\partial s^2}]^2 ds \tag{5.23}$$

and EI denotes the appendage flexural rigidity. Here we have treated each appendage as a "simple" (Euler-Bernouli) beam ignoring shear deformation and other higher order effects, except we have retained the rotational stiffening term as one representative nonlinearity to demonstrate methods for dealing with nonlinear effects in optimal maneuver and vibration arrest problems.

By a direct application of Hamilton's principle using Eqs. 5.12, 5.21, and 5.22, one can obtain the governing nonlinear system of integro-partial differential equations which describe the motion. However, the resulting integro-partial differential equation system model is difficult to deal with either analytically or numerically (see ref. 5.2 for a convolution integral method for solving the linear partial differential equations governing the motion of the vehicle). We discuss in the next section several methods which have proven useful for obtaining an approximate system of ordinary differential equations to describe the motion for a relatively wide class of structures.

5.4 APPROXIMATE DISCRETIZATION METHODS FOR DISTRIBUTED PARAMETER SYSTEMS

We assume in this section that the partial differential equation of motion governing the response of a distributed parameter system is sufficiently complex that an exact solution does not exist, or is not feasible*. As a result, we are forced to use approximate equations of motion.

In each of the approximation techniques considered in this section, we employ a spatial discretization, whereby we replace the continuous elastic systems approximately by discrete systems. Two spatial discretization methods

*References 46 and 49 contain excellent surveys of the family of problems which can be solved rigorously without discretization.

are briefly discussed. The two methods are known as (1) the assumed modes method, and (2) the finite element method. The assumed modes approach is useful for problems whose geometry is sufficiently simple to permit the insight necessary to select a "good" set of global displacement functions. The finite element approach, on the other hand, is more broadly applicable to near-arbitrary geometries.

5.4.1 The Assumed Modes Method

In the assumed modes method, the continuous elastic structures are replaced by a finite series of space-dependent functions which are multiplied by time-dependent functions. The space dependent functions are typically selected to satisfy geometric boundary conditions such as zero displacement and zero slope at the attach points between contiguous bodies. In addition, if the problem formulation and a priori insight permits, the space-dependent functions may also be selected to satisfy physical (natural) boundary conditions such as zero shear and zero moment at the ends of unconstrained bodies. In practice the selected space-dependent functions will not in general satisfy the spatial differential equation resulting from a separation of variables technique for the governing partial differential equation (i.e., the assumed modes are generally <u>not</u> the linearized system eigenfunctions, although the system eigenfunctions, if available, would be a delightfully attractive admissible set of assumed modes!). The assumed modes method has a misleading name, since it is *not* assumed that the "assumed modes" are the normal modes or eigenfunctions of the system under consideration, however, the eigenfunctions are approximated by linear combinations of the assumed modes.

Selecting the assumed modes as approximate mode shapes, however, is useful due to the properties of the *Rayleigh's quotient*, given by

$$\lambda = \omega^2 = \frac{\{u\}^T[K]\{u\}}{\{u\}^T[M]\{u\}} \tag{5.24}$$

where [M] is the mass matrix, [K] is the stiffness matrix, $\{u\}$ is an arbitrary vector, and ω is the associated natural frequency. In particular, it can be shown (refs. 46 and 49) that the quotient has stationary values if $\{u\}$ is chosen as one of the system eigenvectors. Moreover, it follows that when the vector $\{u\}$ deviates from a system eigenvector by a small amount, e.g., $\{\varepsilon\}$, such that

$$\{u\} \stackrel{\Delta}{=} \{u_r\} + \{\varepsilon\} \tag{5.25}$$

where $\{u_r\}$ denotes the rth system eigenvector; then Rayleigh's quotient yields an *upper bound* estimate for the rth natural frequency, i.e.

$$\omega^2 = \omega_r^2 + O(\varepsilon^2) \tag{5.26}$$

where $O(\varepsilon^2)$ denotes positive errors of order $\{\varepsilon\}^T\{\varepsilon\}$.

We observe, however, that the quotient above is given for discrete systems; nevertheless, the generalization for the continuous system is easily obtained when we recognize the system kinetic and potential energies (of harmonic motion) are contained in the quotient as follows:

$$2V = \{u\}^T[K]\{u\}$$

$$2T = \{u\}^T[M]\{u\}\omega^2$$

where V is the potential energy and T is the kinetic energy.

Thus, the correct form for Rayleigh's quotient for continuous systems follows by replacing V and T in the above discussion by their associated integral representations, and the elastic deformation vector $\mathbf{u}(x,y,z,t)$ by the approximation

$$\mathbf{u}(x,y,z,t) = [\phi(x,y,z)]\eta(t) \tag{5.27}$$

where, for example

$$[\phi(x,y,z)] = \begin{bmatrix} \phi_{11}(x,y,z) & \dots & \phi_{1n}(x,y,z) \\ \phi_{21}(x,y,z) & \dots & \phi_{2n}(x,y,z) \\ \phi_{31}(x,y,z) & \dots & \phi_{3n}(x,y,z) \end{bmatrix}, \tag{5.28}$$

is a 3xn spatial operator whose elements are the assumed shape functions; η is a set of n x 1 time varying amplitudes (generalized coordinates) which interpolate the instantaneous spatial deformation, and $\phi_{ij}(x,y,z)$ denotes the (i,j)th assumed shape functions for the x, y, z deformation coordinates. Indeed, the success of each of the approximate methods discussed in this section depends implicitely upon the special properties of Rayleigh's quotient.

5.4.1.1 Assumed Modes Application for a Simple Structure

As an illustration of the procedure for linear elastic systems; we have (upon introducing the assumed form of the elastic deformation coordinates into the integral expression for the kinetic energy), the following series expression:

$$T(t) = \frac{1}{2}\int_V (\dot{u}_x^2 + \dot{u}_y^2 + \dot{u}_z^2)\rho dv = \frac{1}{2}\sum_{i=1}^{n}\sum_{j=1}^{n} m_{ij}\dot{\eta}_i(t)\dot{\eta}_j(t) \qquad (5.29)$$

where m_{ij} denotes the (i,j)th symmetric mass matrix coefficient which depends on the mass distribution of the system and the assumed mode shapes $\phi_{ij}(x,y,z)$. In an analogous way, the potential energy can be developed as the quadratic form

$$V(t) = \frac{1}{2}\sum_{i=1}^{n}\sum_{j=1}^{n} k_{ij}\eta_i(t)\eta_j(t) \qquad (5.30)$$

where k_{ij} denotes the (i,j)th symmetric stiffness matrix coefficient which depends on the stiffness distribution and the assumed mode shapes. The kinetic and potential energy expressions in Eqs. 5.29 and 5.30, however, do not account for rotational/translational coupling effects, so the present discussion represents a simplified example.

The equations of motion follow upon introducing T and V into Lagrange's equations in the form

$$\frac{d}{dt}\left(\frac{\partial T}{\partial \dot{\eta}_r}\right) - \frac{\partial T}{\partial \eta_r} + \frac{\partial V}{\partial \eta_r} = Q_r \quad , \quad r = 1,2,\ldots,n \qquad (5.31)$$

where Q_r denotes the generalized nonconservative forces which can be obtained from Eq. 5.8.

Substituting Eqs. 5.29 and 5.30 into Eq. 5.31, leads to

$$\sum_{j=1}^{n} m_{rj}\ddot{\eta}_j(t) + \sum_{j=1}^{n} k_{rj}\eta_j(t) = Q_r \quad , \quad r = 1,\ldots,n \tag{5.32}$$

which can be written in the matrix form

$$[M]\{\ddot{\eta}(t)\} + [K]\{\eta(t)\} = \{Q\} \tag{5.32}$$

Equation 5.32 provides the desired equation of motion in terms of the assumed mode amplitudes and their time derivatives. The time history for the configuration vector $\{\eta(t)\}$ follows upon prescribing $\{\eta(t_o)\}$ and $\{\dot{\eta}(t_o)\}$, and pre-multiplying Eq. 5.32 by $[M]^{-1}$; thus, at least formally, yielding the acceleration vector $\{\ddot{\eta}(t)\}$ which can be integrated to produce the velocity $\{\dot{\eta}(t)\}$ and position $\{\eta(t)\}$. Alternatively, we can introduce a *modal coordinate transformation* which simultaneously diagonalizes [M] and [K]; thus yielding uncoupled equations for the system accelerations. In practice, the latter option proves to be advantageous both analytically and computationally, for the most common case of constant coefficient dynamical systems.

In order to illustrate the technique, we now introduce in Eq. 5.32 the diagonalizing coordinate transformation

$$\{\eta(t)\} = [U]\{q(t)\} \tag{5.33}$$

where [U] denotes the constant normalized eigenvector matrix ("modal matrix") for the generalized eigenvalue problem

$$[K]\{u^r\} = \Lambda_r[M]\{u^r\} \quad , \quad \Lambda_r = \omega_r^2 \; (r = 1,\ldots,n) \tag{5.34}$$

and

$\{q\}$ is an n x 1 vector of *modal coordinates*

$[U] = [\{u^1\}\{u^2\} \ldots \{u^n\}]$, the modal transformation matrix

$\{u^r\}$ denotes the rth eigenvector

$\Lambda_r = \omega_r^2$ denotes the rth eigenvalue

The transformed generalized coordinates $\{q(t)\}$ of Eq. 5.33 are referred to as normal or modal coordinates. The eigenvector matrix $[U]$ is usually normalized with respect to the mass matrix so the *orthogonality conditions* assume the form

$$[U]^T[M][U] = [I] \tag{5.35}$$

and

$$[U]^T[K][U] = [\Lambda] \tag{5.36}$$

where $[\Lambda] = \text{Diag.}[\Lambda_1,\ldots,\Lambda_n] = \text{Diag.}[\omega_1^2,\ldots,\omega_n^2]$.

Introducing Eq. 5.33 into Eq. 5.32 and pre-multiplying by $[U]^T$, leads to the set of uncoupled equations of motion given by

$$\{\ddot{q}(t)\} + [\Lambda]\{q(t)\} = [U]^T\{Q\} \tag{5.37}$$

where it follows from Eqs. 5.33 and 5.35* that the initial conditions for Eq. 5.37 are given by

$$\{q(t_o)\} = [U]^T[M]\{\eta(t_o)\} \tag{5.38}$$

and

$$\{\dot{q}(t_o)\} = [U]^T[M]\{\dot{\eta}(t_o)\} \tag{5.39}$$

The time response of the original system follows by integrating Eq. 5.37 subject to the initial conditions provided by Eqs. 5.38 and 5.39; obtaining $\{\eta(t)\}$ from $\{q(t)\}$ via Eq. 5.33; and introducing $\{\eta(t)\}$ into Eq. 5.28, thus yielding the elastic deformation vector $\mathbf{u}(x,y,z,t)$ as a function of time throughout the elastic domain.

The relationship between the assumed modes method above and the Rayleigh-Ritz method can be traced to Eq. 5.34. Indeed, if we use the assumed modes of Eq. 5.28 and attempt to determine the stationary values of Rayleigh's quotient, we arrive at precisely the eigenvalue problem defined by Eq. 5.34. Thus we know that the squares of the system frequencies given by Λ_i for $i = 1,\ldots,n$ in

---

*e.g., it follows that $[U]^{-1} = [U]^T[M]$, as a consequence of the generalized orthogonality condition of Eq. 5.35.

Eq. 5.36 represent upper bound estimates of the first n eigenvalues of the continuous system. Furthermore, we find that the estimated eigenfunctions are approximated by linear combination of the "assumed modes" as

$$u_j^{(r)}(x,y,z) = \sum_{i=1}^{n} \{u^r\}_i \phi_{ji}(x,y,z) \quad , \quad j = 1,2,3$$

where $\{u^r\}_i$ denotes the ith element of the vector $\{u^r\} = \{u_1^r u_2^r \ldots u_n^r\}^T$. Thus, the use of uncoupled coordinates provides us with valuable physical insight into the response of the continuous system, as well as significant computational advantages.

5.4.1.2 Assumed Mode Application for a Rotating Spacecraft

If higher order nonlinear effects are retained in the kinetic and potential energy expressions, it is frequently advantageous to retain the original system of coupled differential equations; since the presence of nonlinear effects does not readily permit an uncoupling transformation to be carried out.

To illustrate the procedure, we consider the vehicle depicted in Figure 5.1, where the kinetic energy is given by Eq. 5.21 and the potential energy is given by Eq. 5.22. Moreover, since only transverse deflections are considered, we assume that the elastic deflection coordinate u(s,t) is given by

$$u(s,t) = \sum_{i=1}^{m} \phi_i(s)\eta_i(t) \tag{5.40}$$

where $\phi_i(s)$ denotes the ith assumed mode shape and $\eta_i(t)$ denotes the ith generalized coordinate defining the time response of the system. Thus, the system kinetic energy is given by

$$T = \frac{1}{2}(I_{Hub} + 4I_{Appendage})\dot{\theta}^2$$

$$+ \frac{1}{2}\dot{\theta}^2 \sum_{i=1}^{n}\sum_{j=1}^{n} \{M_{ij} - \mathbf{M}_{ij}\}\eta_i\eta_j$$

$$+\frac{1}{2}\sum_{i=1}^{n}\sum_{j=1}^{n} M_{ij}\dot{\eta}_i\dot{\eta}_j + \dot{\theta}\sum_{i=1}^{n} \mathbf{M}_{\theta\eta_i}\,\dot{\eta}_i \tag{5.41}$$

where

$$I_{\text{Appendage}} = \rho\int_{r}^{r+L} s^2 ds = m\,\frac{(r+L)^3 - r^3}{3L} \quad ; \quad m = \rho L$$

$$M_{ij} = 4\rho\int_{r}^{r+L} \phi_i(s)\phi_j(s)ds$$

$$\mathbf{M}_{ij} = 4\rho\int_{r}^{r+L} [(r+L)^2 - s^2]\,\frac{\partial\phi_i}{\partial s}\,\frac{\partial\phi_j}{\partial s}\,ds$$

$$M_{\theta\eta_i} = 4\rho\int_{r}^{r+L} s\phi_i(s)ds$$

In an analogous way, the system potential energy is given by

$$V = \frac{1}{2}\sum_{i=1}^{n}\sum_{j=1}^{n} K_{ij}\eta_i\eta_j \tag{5.42}$$

where

$$K_{ij} = 4EI\int_{r}^{r+L} \frac{\partial^2\phi_i}{\partial s^2}\,\frac{\partial^2\phi_j}{\partial s^2}\,ds$$

In the equations above, upon selecting the functional form of $\phi_i(s)$ for $i = 1,\ldots,n$, the integral expressions for the time-invariant matrix elements M_{ij}, $\mathbf{M}_{ij}$, $M_{\theta\eta_i}$, and K_{ij} can be evaluated either analytically or numerically.

In matrix form Eqs. 5.41 and 5.42 can be written as

$$T = \frac{1}{2}\,(I_{\text{Hub}} + 4I_{\text{Appendage}})\dot{\theta}^2 + \frac{1}{2}\,\dot{\theta}^2\{\eta\}^T[M - \mathbf{M}]\{\eta\}$$

$$+\frac{1}{2}\,\{\dot{\eta}\}^T[M]\{\dot{\eta}\} + \dot{\theta}\{M_{\theta\eta}\}^T\{\dot{\eta}\} \tag{5.43}$$

and

$$V = \frac{1}{2}\,\{\eta\}^T[K]\{\eta\} \tag{5.44}$$

In Chapter 9, Eqs. 5.43, 5.44 are used to obtain the equations of motion for the vehicle of Figure 5.1. We observe, however, that the equations of motion obtained from introducing Eqs. 5.43 and 5.44 into Eq. 5.31 are nonlinear; due to the presence of the second term in Eq. 5.43.

On the other hand, if we are solely interested in obtaining information about the vehicle frequencies and mode shapes, we delete the second term in Eq. 5.43 leading to kinetic and potential energy expressions of the form:

$$T = \frac{1}{2}\{\dot{x}\}^T[M^*]\{\dot{x}\} \quad , \quad V = \frac{1}{2}\{x\}^T[K^*]\{x\}$$

$$\{x\} = \begin{Bmatrix} \theta \\ \cdots \\ \{\eta\} \end{Bmatrix} \quad , \quad [M^*] = \left[\begin{array}{c:c} I_{hub} + 4I_{appendage} & \{M_{\theta\eta}\}^T \\ \hdashline \{M_{\theta\eta}\} & [M] \end{array}\right]$$

$$[K^*] = \left[\begin{array}{c:c} 0 & \{0\}^T \\ \hdashline \{0\} & [K] \end{array}\right]$$

These, in turn, lead to the linear differential equation

$$[M^*]\{\ddot{x}\} + [K^*]\{x\} = [P]\{\gamma\}$$

where

$$\{\gamma\} = \begin{Bmatrix} u_r \\ \hdashline \bar{u}_{e1} \\ \hdashline \vdots \\ \hdashline \bar{u}_{en} \\ \hdashline F \end{Bmatrix} \quad ; \quad P = \begin{bmatrix} 1 & 4 & \cdots & 4 & 4(r+L) \\ 0 & 4\phi^1_{1,x} & \cdots & 4\phi^n_{1,x} & 4\phi_1 \\ \vdots & \vdots & & \vdots & \vdots \\ 0 & 4\phi^1_{n,x} & \cdots & 4\phi^n_{n,x} & 4\phi_n \end{bmatrix}$$

$$\phi^j_{r,x} = \left.\frac{\partial \phi_r}{\partial x}\right|_{x_{ej}}$$

where P is obtained by linearizing Eq. 5.12. The approximate vehicle natural frequencies and mode shapes are found upon introducing a diagonalizing transformation of the form of Eq. 5.33.

In summary, the assumed modes method provides a means for analyzing dynamically deforming elastic bodies; this proves especially attractive for the case in which approximate mode shapes are available. For more complex structural designs, however, we usually find other, more general modeling techniques to be advantageous. In the next section we briefly describe the finite element method, which represents a very general family of modeling techniques.

5.4.2 The Finite Element Method

Given the many design constraints placed on space missions, and the often ad hoc fashion by which spacecraft designs evolve, it is not surprising that the geometric shapes of many vehicles are rather complex, irregular, and composed of many interconnected parts which, taken as a system defy simple analytical characterization. Thus, there is ample motivation for using general-purpose modeling techniques which can be used to analyze a wide range of vehicle configurations. For this reason, finite element methods enjoy an dominant role in structural analysis for static deformation, dynamics, and control. In the finite element approach, the vehicle structure is regarded as an assembly of many discrete elements, where each element locally models a portion of the domain. The family of piecewise continuous elements constitutes a finite element model. Consequently, the finite element method represents a spatial discretization. The nature of the local interpolation functions, the size of the finite elements, and the degree of inter-element continuity interact in a relatively complicated way to affect the precision of this approach.

The entire structure is required to move in unison by imposing rotational, translational, and continuity constraints at the joints and boundaries between contiguous elements; in addition, the internal forces are required to balance at the joints (refs. 46, 47, 48, and 49). Consequently, the finite element method expresses the displacement of any point in a structure as a function of a finite number of displacements, usually at the boundaries of the elements.

The flexibility of the method lies in the fact that the analyst is free to specify and vary the degree of modeling complexity in the various subsystems which comprise the vehicle. For example, if the vehicle possesses substructures which can be modeled as essentially rigid, very few elements are required; whereas if flexible antennas, solar shields, or solar arrays are involved, many elements may be required for these subsystems. Of course, the extent of modeling required at the subsystem level is fundamentally (and often, intuitively) guided by the influence which a particular subsystem has on the overall system response and performance. Numerical experiments are usually used to refine the modeling details and gain confidence that, for example, the number of elements is sufficient for the problem at hand.

The major drawback of the finite element approach is that many degrees of freedom may be required in order to obtain a reasonable representation for the structure's deflection. In fact, it is not unusual for several thousand degrees of freedom to be required in a finite element model, but fortunately, we are only (typically) concerned with a few tens of the resulting normal modes of vibration. It is of interest to note that we have found the assumed modes method (for moderately complicated structures) usually converges with many fewer degrees of freedom than a finite element representation of the same structure. Nevertheless, this statement is rather dependent upon the particular structure and does not generalize to complicated structures due to the difficulty of assuming judicious "assumed modes". Fortunately, many finite element computer codes are available which automate the finite element technique (e.g., NASTRAN, SPAR, and others).

For a typical spacecraft modeling problem, the system natural frequencies and corresponding eigenvectors or mode shapes are among the most important final results of a finite element analysis. For example, using the mode shape information, it becomes possible to evaluate the integral expressions in Eqs. 5.41 and 5.42; thus yielding the (generally nonlinear) equations of motion. Indeed, in Reference 21, a computer program known as DISCOS is discussed, this program has the capability of carrying out nonlinear simulations for vehicles consisting of n flexible substructures, where each substructure has an independent finite element description. Each substructure may undergo large, nonlinear rigid body motions, however the structural deformations must remain small enough (as seen from sub-structure-fixed reference frame) to justify linear stress-strain approximations. Although a complete treatment of the DISCOS methodology is outside the scope of the present discussion, a brief summary of the equations of motion is given below. Our objective here is to provide some insight into the structure of the equations of motions for a general-purpose multibody modeling approach.

5.4.2.1 Multibody Spacecraft Equations of Motions Requiring Sub-Structure Finite Element Models

Central to the DISCOS analysis approach is the fact that the displacement and deformation of each body is modeled individually and the composite system response is achieved by enforcing rotational and translational velocity constraints at the interconnection hinges between contiguous bodies. The constraint forces and torques are computed by using the Lagrange multiplier method discussed in Section 3.2.5. The great power and versatility of the method comes about because the Lagrange multiplier vector, for the constrained system accelerations, is computed as the noniterative solution of a linear algebraic equation. The system equations of motion follow as:

$\{\dot{U}\}_j = [M]_j^{-1}(\{G\} + [b]_j^T\{\lambda\})$

$\{U\}_j = (\omega_x, \omega_y, \omega_z, u, v, w, \dot{\xi}_1, \ldots, \dot{\xi}_{Nj})_j^T$

$=$ jth body velocity state

$(\omega_x, \omega_y, \omega_z)$ = denote the body components of angular velocity for the jth body (quasi-coordinates)

(u, v, w) = denote the body components of the jth body reference point inertial velocity (quasi-coordinates)

$(\dot{\xi}_1,\ldots,\dot{\xi}_{Nj})$ = denote the N_j generalized coordinates for the elastic structural deformations of the jth body, where the elastic displacement vector $\mathbf{u}(x,y,z,t)$ is given by $\mathbf{u}(x,y,z,t)=[\phi_{xk}(x,y,z)\hat{\mathbf{b}}_1+\phi_{yk}(x,y,z)\hat{\mathbf{b}}_2+\phi_{zk}(x,y,z)\hat{\mathbf{b}}_3]\xi_k$*

$(\phi_{xk},\phi_{yk},\phi_{zk})$ = displacement functions which are provided at a discrete set of points in a finite element representation of the elastic continuum for an individual body

$[M]_j$ = time-varying mass matrix for the jth body

$$
= \begin{bmatrix}
J_{xx} & J_{xy} & J_{xz} & 0 & -S_z & S_y & d_{x1} & d_{x2} & \cdots & d_{xNj} \\
 & J_{yy} & J_{yz} & S_z & 0 & -S_x & d_{y1} & d_{y2} & \cdots & d_{yNj} \\
 & & J_{zz} & -S_y & S_x & 0 & d_{z1} & d_{z2} & \cdots & d_{zNj} \\
 & & & m & 0 & 0 & a_{x1} & a_{x2} & \cdots & a_{xN_j} \\
 & & & & m & 0 & a_{y1} & a_{y2} & \cdots & a_{yN_j} \\
 & & & & & m & a_{z1} & a_{z2} & \cdots & a_{zN_j} \\
 & & & & & & e_{11} & e_{12} & \cdots & e_{1N_j} \\
\text{sym.} & & & & & & & e_{22} & \cdots & e_{2N_j} \\
 & & & & & & & & \ddots & \vdots \\
 & & & & & & & & & e_{N_jN_j}
\end{bmatrix}_j
$$

m = mass of the jth body

$$= \int_V \rho dV$$

J_{xx}

$$= \int_V [(y + \phi_{yj}\xi_j)^2 + (z + \phi_{zj}\xi_j)^2]\rho dv$$

$$= J_{xxo} + 2(b_{yyj} + b_{zzj})\xi_j + (C_{yjyk} + C_{zjzk})\xi_j\xi_k$$

*Note summation convention:

$$\phi_{xk}\xi_k \equiv \sum_{k=1}^{N} \phi_{xk}\xi_k.$$

$$b_{yyj} = \int_v y\phi_{yj}\rho dv$$

$$b_{zzj} = \int_v z\phi_{zj}\rho dv$$

$$C_{yjzk} = \int_v \phi_{yj}\phi_{zk}\rho dv$$

$$a_{xk} = \int_v \phi_{xk}\rho dv$$

$$e_{jk} = \int_v (\phi_{xj}\phi_{xk} + \phi_{yj}\phi_{yk} + \phi_{zj}\phi_{zk})\rho dv$$

$$S_x = \int_v (x + \phi_{xj}\xi_j)\rho dv$$

$$= a_{xo} + a_{xj}\xi_j$$

$$d_{xk} = \int_v [(y + \phi_{yj}\xi_j)\phi_{zk} - (z + \phi_{zj}\xi_j)\phi_{yk}]\rho dv$$

$$= b_{yzk} - b_{zyk} + (C_{yjzk} - C_{zjyk})\xi_j$$

$$J_{xy} = \int_v (x + \phi_{xj}\xi_j)(y + \phi_{yj}\xi_j)\rho dv$$

$$= J_{xyo} + (b_{xyj} + b_{yxj})\xi_j + C_{xjyk}\xi_j\xi_k{}^{+}$$

$$\{G\}_j = \{G_{ex}\}_j - [-\tfrac{0}{K}-]_j\{\xi\}_j - [-\tfrac{0}{C}-]_j\{\dot{\xi}\}_j$$
$$+ [\tilde{\Omega}]_j[M]_j\{U\}_j + \frac{1}{2}\{U\}_j^T[M,r]\{U\}_j\}$$
$$- [\dot{M}]_j\{U\}_j$$

$\{G_{ex}\}_j$ = all external forces and torques acting on the jth body, resolved about the jth body reference point

$[K]_j$ = stiffness matrix for the jth body

$[C]_j$ = damping matrix for the jth body

[+]All other quantities involved in the system mass matrix are obtained by a cyclic permutation of the indices x, y, z in the inertial integral definitions for the a, b, and c coefficients.

$$[\tilde{\Omega}]_j = \left[\begin{array}{ccc|ccc|c} 0 & \omega_z & -\omega_y & 0 & w & -v & \\ -\omega_z & 0 & \omega_x & -w & 0 & u & 0_{3xN_j} \\ \omega_y & -\omega_x & 0 & v & -u & 0 & \\ \hline & & & 0 & \omega_z & -\omega_y & \\ & 0_{3x3} & & -\omega_z & 0 & \omega_x & 0_{3xN_j} \\ & & & \omega_y & -\omega_x & 0 & \\ \hline & 0_{N_jx3} & & & 0_{N_jx3} & & 0_{N_jxN_j} \end{array}\right]_j$$

$[M,r]_j$ = the partial derivative of each element of $[M]$ with respect to the rth generalized coordinate.

$[\dot{M}]_j$ = the time derivative of the jth body mass matrix.

$\{\lambda\}$ = Lagrange multiplier vector

$[b]_j$ = operator matrix which transforms the Lagrange multipliers into constraint forces and torques acting at the jth body reference point.

Kinematics:

Elastic Deformations

$\{\dot{\xi}\}_j$ = $[S_\xi]_j\{U\}_j$

$[S_\xi]_j$ = constant selection operator matrix for the generalized elastic deformation coordinates

Independent System Degrees of Freedom

$$\{\dot{\beta}\} = \sum_{j=1}^{N_B} [B]_j\{U\}_j$$

$[B]_j$ = operator matrix which transforms the jth body velocity state into independent system degrees of freedom (i.e., relative translation and rotation rates across interconnection hinges between contiguous bodies)

N_B = number of bodies

Control Differential Equations

$$\{\dot{\zeta}\} = f(\{\beta\},\{\dot{\beta}\},\{\xi\},\{\dot{\xi}\},\{\zeta\}) \quad , \text{ user specified.}$$

Constraint Differential Equations

$$\{\dot{\alpha}\} = \sum_{j=1}^{N_B} [b]_j\{U\}_j,$$ a vector of user specified $\{\dot{\alpha}\}$ velocity constraints across hinges connecting contiguous bodies.

The solution for the Lagrange multiplier vector is obtained by differentiating the constraint differential equations with respect to time, yielding:

$$\{\ddot{\alpha}\} = \sum_{j=1}^{N_B} [\dot{b}]_j\{U\}_j + \sum_{j=1}^{N_B} [b]_j\{\dot{U}\}_j$$

By introducing the dynamics equation for $\{\dot{U}\}_j$ above, we obtain

$$\{\ddot{\alpha}\} = \sum_{j=1}^{N_B} [\dot{b}]_j\{U\}_j + \sum_{j=1}^{N_B} [b]_j[M]_j^{-1}(\{G\}_j + [b]_j^T\{\lambda\})$$

which can be solved for the Lagrange multiplier vector, yielding:

$$\{\lambda\} = \Big(\sum_{j=1}^{N_B} [b]_j[M]_j^{-1}[b]_j^T\Big)^{-1}\Big[\{\ddot{\alpha}\} - \sum_{j=1}^{N_B} \big([\dot{b}]_j\{U\}_j + [b]_j[M]_j^{-1}\{G\}_j\big)\Big]$$

By introducing the numerical solution for $\{\lambda\}$ into the constrained accelerations for the jth body, the system response can now be integrated. For a complete specification of the $[b]_j$, $[\dot{b}]_j$, and $[B]_j$ matrices, the reader is directed to Reference 21. Of course other forms for the equations of motion for coupled dynamical systems are possible, however, the method presented above turns out to be particularly simple to implement.

5.2.2.2 Finite Element Models: A Simplified Example

In the above discussion, we do not consider the details of the implicit finite element model which is required for each elastic member of the multibody system.

Since the finite element method is a broadly used family of techniques in engineering and applied mathematics (ref. 47) we make no attempt here to provide a detailed treatment dealing with the many special features of this broad family. Instead, we concern ourselves with a simple application which highlights the conceptual essence of the approach.

To this end, we derive the equations of motion for the rod shaped element shown in Figure 5.4*. The problem is simplified in the sense that it is one-dimensional and the joints consist of the two end points. The element is of length L, linear mass density m, cross-sectional area A, and possesses a modulus of elasticity E, where L, m, A, and E are assumed to be constants. The axial displacement is assumed to be given by

$$u(x,t) = \phi_1(x)u_1(t) + \phi_2(x)u_2(t) \tag{5.45}$$

where $\phi_1(x)$ and $\phi_2(x)$ are the so-called "shape functions" which must be selected to satisfy prescribed boundary conditions. From Figure 5.4 it follows that $u(x,t)$ must be selected such that

$$u(0,t) = u_1(t) \quad , \quad u(L,t) = u_2(t) \tag{5.46}$$

Subject to Eq. 5.46, considering the simplest possible case of a single element model, it follows from Eq. 5.45 that $\phi_1(x)$ and $\phi_2(x)$ must satisfy the boundary conditions

$$\phi_1(0) = 1 \quad , \quad \phi_1(L) = 0 \tag{5.47}$$

$$\phi_2(0) = 0 \quad , \quad \phi_2(L) = 1 \tag{5.48}$$

*This example is based upon Reference 49, pg. 288-290.

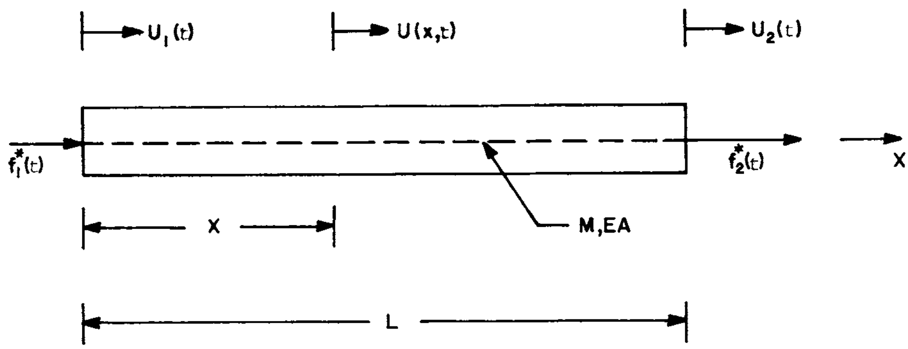

Figure 5.4 Finite Element Free Body Diagram

The simplest interpolation functions we can select are linear polynomials of the form

$$\phi_i(x) = C_{1i} + C_{2i}x \quad , \quad i = 1,2 \tag{5.49}$$

Upon evaluating the constants in Eq. 5.49, subject to the boundary conditions of Eqs. 5.47 and 5.48, we find

$$\phi_1(x) = 1 - \frac{x}{L} \quad , \quad \phi_2(x) = \frac{x}{L} \tag{5.50}$$

From which it follows that u(x,t) is approximated by the linear interpolation

$$u(x,t) = (1 - \frac{x}{L})u_1(t) + \frac{x}{L}\, u_2(t) \tag{5.51}$$

To obtain the equations of motion for the element using a Lagrangian formulation, we first consider the kinetic energy from the definition

$$T \cong \frac{1}{2}\int_0^L m[\frac{\partial u(x,t)}{\partial t}]^2 dx$$

Thus

$$T = \frac{1}{2}\int_0^L m[(1 - \frac{x}{L})\dot{u}_1(t) + \frac{x}{L}\,\dot{u}_2(t)]^2 dx$$

or

$$T = \frac{1}{2}\frac{mL}{3}\,[\dot{u}_1^2(t) + \dot{u}_1(t)\dot{u}_2(t) + \dot{u}_2^2(t)] \tag{5.52}$$

Similarly, the potential energy is given by

$$V = \frac{1}{2}\int_0^L EA\left[\frac{\partial u(x,t)}{\partial x}\right]^2 dx$$

or

$$V = \frac{1}{2}\int_0^L EA\left[-\frac{1}{L}\,u_1(t) + \frac{1}{L}\,u_2(t)\right]^2 dx$$

then

$$V = \frac{1}{2}\frac{EA}{L}\,[u_1^2(t) - 2u_1(t)u_2(t) + u_2^2(t)] \tag{5.53}$$

To compute the generalized forces associated with the generalized coordinates $u_1(t)$ and $u_2(t)$, we use virtual work expression of Eq. 5.2, repeated here as

$$\delta W = \sum_{k=1}^{n} Q_k\,\delta q_k$$

where Q_k is given by Eq. 5.8. Observing that $\mathbf{R} = \dot{\mathbf{R}} = \omega = \mathbf{0}$ in Eq. 5.8 for the problem at hand, it follows that Q_k can be written as

$$Q_k = \int_0^L \frac{\partial \dot{u}(x,t)}{\partial \dot{q}_k}\cdot \mathbf{df}$$

$$Q_k = \int_0^L \left[\left(1 - \frac{x}{L}\right)\frac{\partial \dot{u}_1(t)}{\partial \dot{q}_k} + \left(\frac{x}{L}\right)\frac{\partial \dot{u}_2(t)}{\partial \dot{q}_k}\right] df,$$

so

$$Q_k = f_1(t)\,\frac{\partial \dot{u}_1(t)}{\partial \dot{q}_k} + f_2(t)\,\frac{\partial \dot{u}_2(t)}{\partial \dot{q}_k} \tag{5.54}$$

where we made use of

$$df = [f(x,t) + f_1^*(t)\delta(x) + f_2^*(t)\delta(x - L)]dx$$

$$f_1(t) = \int_0^L f(x,t)(1 - \frac{x}{L})dx + f_1^*(t)$$

$$f_2(t) = \int_0^L f(x,t)(\frac{x}{L})dx + f_2^*(t)$$

$f(x,t)$ = distributed external nonconservative force

$f_i^*(t)$ = external point force at the ith joint

$\delta(\cdot)$ = Dirac delta function

$$\frac{\partial \dot{u}_i(t)}{\partial \dot{q}_k} = \begin{cases} 1 & i = k \\ 0 & i \neq k \end{cases}$$

Introducing Eq. 5.54 into Lagrange's equation, leads to the standard form

$$[M]\{\ddot{u}(t)\} + [K]\{u(t)\} = \{f(t)\} \tag{5.55}$$

where

$$\{u(t)\} = \begin{Bmatrix} u_1(t) \\ u_2(t) \end{Bmatrix} , \quad \{f(t)\} = \begin{Bmatrix} f_1(t) \\ f_2(t) \end{Bmatrix}$$

$$[M] = \frac{mL}{6}\begin{bmatrix} 2 & 1 \\ 1 & 2 \end{bmatrix} , \quad [K] = \frac{EA}{L}\begin{bmatrix} 1 & -1 \\ -1 & 1 \end{bmatrix}$$

Once $\{u(t_o)\}$ and $\{\dot{u}(t_o\}$ have been specified, the complete time history for the response $u(x,t)$ follows upon integrating Eq. 5.55.

If the element in Figure 5.4 is permitted to deform in the y direction as well as rotate at the joints, the assumed form for the displacement interpolation contains as many shape functions as there are degrees of freedom. By imposing the requisite boundary conditions on the displacement function, one can find the associated boundary conditions for the shape functions which in turn permit a solution for the coefficients in the shape functions. As above, with appropriate shape functions prescribed, the equations of motion can be obtained.

To make these concepts useful for space structures, the one-dimensional element ideas of this section, of course, must be generalized to two- and three-dimensional discrete elements. Likewise, the number of elements can (and must) be increased to decrease the truncation errors implicit in this process. These generalizations are largely straightforward, however, they are outside the scope of the present discussion. An excellent exposition of the general theory can be found in Reference 47.

REFERENCES

1. W. Hooker, and G. Margulies, "The Dynamical Attitude Equations for an n-body Satellite," **J. Astronautical Science**, Vol. 12, pp. 123-128, 1965.

2. R. Roberson and J. Wittenburg, "A Dynamical Formalism for an Arbitrary Number of Interconnected Rigid Bodies with Reference to the Problem of Satellite Attitude Control," in **Proceedings of the Third International Congress of Automatic Control** (London, 1966), Butterworth and Co., Ltd., London, 1967..

3. H. Fletcher, L. Rongved and E. Yu, "Dynamic Analysis of a Two-Body Gravitational Oriented Satellite," **Bell System Technical Journal**, 42, 5, 1963, pp. 2239-2266.

4. C. Gruben, "Dynamics of a Vehicle Containing Moving Parts," **Journal of Applied Mechanics**, Sept. 1962, pp. 486-488.

5. R. Roberson, "Torques on a Satellite Vehicle from Internal Moving Parts," **Journal of Applied Mechanics**, Vol. 25, 1958, pp. 196-200.

6. J. Wittenburg, **Dynamics of Systems of Rigid Bodies**, B. G. Teubner, Stuttgart, 1977.

7. J. Wittenburg, "Dynamics of Multibody Systems," IUTAM (International Union of Theoretical and Applied Mechanics) 1980, pp. 199-207.

8. O. Fischer, **Einführung in die Mechanik lebender Mechanisms**, Leipzig, 1906.

9. W. Russel, "On the Formulation of Equations of Rotational Motion for an N-body Spacecraft," Aerospace Corporation, El Segundo, Calif. Report Tr-0200(4133)-2, 1969, Air Force Report No. SAMSO-TR-69-202.

10. S. Sandler, "Dynamic Equations for Connected Rigid Bodies," **Journal of Spacecraft and Rockets**, Vol. 4, No. 5, May 1967, pp. 684-685.

11. R. Roberson, "Comment on 'Dynamic Equations for Connected Rigid Bodies'," **Journal of Spacecraft and Rockets**, Vol. 4, No. 11, November 1967, p. 1564.

12. P. Likins and P. Wirsching, "Use of Synthetic Modes in Hybrid Coordinate Dynamic Analysis," **AIAA Journal**, 6, 1968, 1867-1872.

13. J. Farrell, J. Newton, and J. Connelly, "Digital Program for Dynamics of Non-Rigid Gravity Gradient Satellites," CR-1119, NASA, Aug. 1968.

14. Hooker, W., "A Set of r Dynamical Attitude Equations for an Arbitrary n-Body Satellite Having r Rotational Degrees of Freedom," **AIAA Journal**, Vol. 8, No. 7, July 1970, pp. 1205-1207.

15. Roberson, R., "A Form of the Translational Dynamical Equations for Relative Motion in Systems of Many Non-Rigid Bodies," **Acta Mech**, 14, 1972, pp. 297-308.

16. Hooker, W., "Equations of Motion for Interconnected Rigid and Elastic Bodies: A Derivation Independent of Angular Momentum," **Celestial Mechanics**, 11, 1975, pp. 337-359.

17. Ho, J., "The Direct Path Method for Deriving the Dynamic Equations of Motion of a Multibody Flexible Spacecraft with Topological Tree Configuration," AIAA Paper 74-786, AIAA Mechanics and Control of Flight Conference, Anaheim, Calif., 1974.

18. Ho, J., "Direct Path Method for Flexible Multibody Spacecraft Dynamics," **Journal of Spacecraft and Rockets**, Vol. 14, Feb. 1977, pp. 102-110.

19. Hughes, P., "Dynamics of a Chain of Flexible Bodies," **Journal of the Astronautical Sciences**, Vol. 27, 1979, pp. 359-380.

20. Likins, P., "Dynamics Analysis of a System of Hinge-Connected Rigid Bodies with Nonrigid Appendages," **International Journal of Solids and Structures**, Vol. 9, 1973, pp. 1473-1487.

21. Bodley, C., A Devers, A. Park, and H. Frisch, "A Digital Computer Program for the Dynamic Interaction Simulation of Controls and Structures (DISCOS)," NASA Technical Paper 1219, May 1978.

22. Boland, P., J. Samin, and P. Willems, "Stability Analysis of Interconected Deformable Bodies in a Topological Tree," **AIAA Journal**, Vol. 12, 1974, pp. 1025-1030.

23. Boland, P., J. Samin, and P. Willems, "Stability Analysis of Interconnected Deformable Bodies in a Closed-Loop Configuration, **AIAA Journal**, Vol. 13, 1975, pp. 864-167.

24. Singh, R., and P. Likins, "Floating Reference Frames for Multi-Flexible-Body," AIAA Paper 81-623.

25. Roberson, R. (ed.), "Lectures on Dynamics of Flexible Spacecraft, Dubrovnik," Sept. 1971, published by Centre Internationale des Sciences Mecaniques, Udine, 1971.

26. Lilov, L., and J. Wittenburg, "Bewegungsgleichungen für Systeme starrer Korper mit Gelenken beliebiger Eigenschaften," **ZAMM** 57, 1977, pp. 137-152.

27. Wittenburg, J., "Nonlinear Equations of Motion for Arbitrary Systems of Interconnected Rigid Bodies," Symposium on Dynamics of Multibody Systems, Munich, Germany, August 28-Sept. 3, 1977. Proceedings published by Springer-Verlag, 1978, K. Magnus, editor.

28. Williams, C., "Dynamics Modelling and Formulation Techiques for Non-Rigid Spacecraft," Paper N76-28303, Symposium on the Dynamics and Control of Non-Rigid Space Vehicles, Frascati, Italy, May 1976.

29. P. Likins, "Analytical Dynamics and Nonrigid Spacecraft Simulation," Tech Report 32-1593, Jet Propulsion Laboratory, Pasadena, Calif., July 15, 1974.

30. T. Kane and Levinson, "Formulation of Equations of Motion for Complex Spacecraft," **Journal of Guidance and Control**, Vol. 3, No. 2, March-April 1980, pp. 99-112.

31. C. Lanczos, **The Variational Principles of Mechanics**, University of Toronto Press, Toronto, Canada, Fourth Edition, 1970.

32. T. Kane, "Dynamics of Nonholonomic Systems," **Journal of Applied Mechanics**, December 1961, pp. 574-578.

33. T. Kane and C. Wang, "On the Derivation of Equations of Motion," **J. Society of Industrial and Applied Mathematics**, Vol. 13, No. 2, June 1965, pp. 487-492.

34. R. Huston and C. Passerello, "On Lagrange's Form of D'Alembert's Principle," **Matrix and Tensor Quarterly**, Vol. 23, No. 3, March 1973, pp. 109-112.

35. C. Bodley and A. Park, "The Influence of Structural Flexibility on the Dynamic Response of Spinning Spacecraft," AIAA Paper 72-348, San Antonio, Texas, 1972.

36. R. Huston and C. Paserello, "On the Dynamics of Chain Systems," American Society of Mechanical Engineers, Paper 74-WA/Aut-11, 1974.

37. R. Huston, C. Passerello, and M. Harlow, "Dynamics of Multibody Systems," **Journal of Applied Mechanics**, Vol. 45, Dec. 1978, pp. 889-894.

38. D. Levinson, "Equations of Motion for Multiple-Rigid-Body Systems via Symbolic Manipulation," **Journal of Spacecraft and Rockets**, Vol. 14, No. 8, August 1977, pp. 479-487.

39. W. Jerkovsky, "The Transformation Operator Approach to Multi-Body Dynamics," Report TR-0076(6901-03)-5, Aerospace Corp., El Segundo, Calif., 1976; also in **The Matrix and Tensor Quarterly**, Part 1 in Vol. 27, Dec. 1976, pp. 48-59; Part 2 in Vol. 27, Jun. 1977, pp. 116-128; Part 3 in Vol. 28, March 1978.

40. W. Jerkovsky, "The Structure of Multibody Dynamics Equations, "**Journal of Guidance and Control**, Vol. 1, No. 3, May-June 1978, pp. 173-182.

41. W. Russell, "Dynamic Analysis of the Communication Satellites of the Future," AIAA Paper No. 76-261, AIAA/CASI 6th Communication Satellite System Conference, Montreal, Canada, April 1976.

42. J. Canavin, "Vibration of a Flexible Spacecraft with Momentum Exchange Controllers," Ph.D. Dissertation, University of California, Los Angeles, June 1976.

43. J. Canavin and P. Likins, "Floating Frames for Flexible Spacecraft," **Journal of Spacecraft and Rockets**, Vol. 14, No. 12, Dec. 1977, pp. 724-732.

44. L. Pars, **A Treatise on Analytical Dynamics**, Oxbow Press, Woodbridge, Connecticut, 1979.

45. J. Baumgarte, "Stabilization of Constraints and Integrals of Motion in Dynamical Systems," **Computer Methods in Applied Mechanics and Engineering**, 1, 1972, pp. 1-16.

46. L. Meirovitch, **Analytical Methods in Vibrations**, The Macmillian Co., New York, 1967.

47. O. C. Zienkiewicz, **The Finite Element Method in Engineering Science**, McGraw-Hill Publishing Company, Ltd., London, 1971.

48. J. S. Przemieniecki, **Theory of Matrix Structural Analysis**, McGraw-Hill Book Co., New York, 1965.

49. L. Meirovitch, **Elements of Vibration Analysis**, McGraw-Hill Publishing Company, New York, 1975.

50. J. W. Strutt (Lord Rayleigh), "On the Theory of Resonance," **Transactions of the Royal Society** (London), Vol. A161, pp. 77-118, 1870.

51. W. Ritz, "Über eine neve Methode zur Lösung Gewissen Variations-Probleme der Mathematischen Physik," **Journal Reine Angew Mathematics**, Vol. 135, pp. 1-61, 1909.

52. S. B. Skaar, and D. Tucker, "The Optimal Control of Flexible Systems Using a Convolution Integral Description of Motion," Proceedings of the 22nd IEEE Conference on Decision and Control, San Antonio, TX, 1983.